DALTON
FULL PAPER

Hydrothermal synthesis, structure, stability and magnetism of $Na_2Co_2(C_2O_4)_3(H_2O)_2$: a new metal oxalate ladder †

Daniel J. Price, Annie K. Powell and Paul T. Wood *‡

School of Chemical Sciences, University of East Anglia, Norwich, UK NR4 7TJ

Received 10th July 2000, Accepted 25th August 2000
First published as an Advance Article on the web 19th September 2000

Purple crystals of the compound $Na_2Co_2(C_2O_4)_3(H_2O)_2$ **1** were synthesized in high yielding hydrothermal reactions. The room temperature crystal structure reveals an anionic cobalt oxalate network with a 2-leg ladder topology. The ladder frameworks run parallel to the *a* axis and are held together by both hydrogen bonding and electrostatic interactions. The magnetism of **1** was studied as a function of temperature and field. The susceptibility shows a broad maximum at about 21 K which is associated with short-range correlations, and a phase transition to a long range ordered Néel state at about 9 K. Above T_N the data are fitted by a range of models which suggests the intra-ladder couplings are of the order -4 to -5 cm^{-1} and the inter-ladder coupling is approximately 0.2 cm^{-1}. Themogravimetric analysis shows **1** to be stable up to 350 °C, where water of crystallisation is lost. A second decomposition episode is seen at 400 °C.

Introduction

Hydrothermal crystallisation is an old technique, having principally been used to obtain synthetic minerals.[1] Recent years have seen a great increase in the popularity of this method to make new inorganic materials.[2] In this class of compounds cobalt carboxylates are particularly well represented. One reason for this success in synthetic inorganic chemistry is that it allows very insoluble compounds to be crystallised.[3] This makes structural characterisation by X-ray crystallography possible facilitating the development of structure–function relationships. The application of such methods to the field of 'molecular' magnetic materials is particularly promising.[4] Whilst magnetic materials is a subject of considerable breadth it is generally true that the most interesting and unusual phenomena occur when there is a strong coupling of the microscopic spin moments. This requires spin carriers to be bridged by ligands that are capable of mediating a significant exchange interaction and often leads to a highly connected network. Such naturally insoluble structures are precisely those well suited to hydrothermal crystallisation methods.

Model magnetic systems and their phase behaviour are still a subject of great theoretical interest in the physics community. Much fundamental work has focused upon universality classes and how order parameter dimensionality controls behaviour.[5] More recently research has focused on the quantum phase behaviour[6] expected in low-dimensional magnetic materials, and how subtle effects such as topology and spin quantum number affect the phase behaviour. Accurate models for the behaviour of simple 1-dimensional magnetic chains have been developed but there are still many unanswered questions concerning 2-dimensional behaviour. These problems are now being approached by considering ladder models,[7] which are intermediate between the 1- and 2-dimensional cases. Testing these models is hampered by a shortage of real examples of spin ladders.[8,9]

We present here the hydrothermal synthesis of a new ternary oxalate. This material is a candidate for a magnetic spin ladder although its structural complexity makes it difficult to compare with existing theoretical results.

† Dedicated to the late Ron Snaith.
‡ Present address: University Chemical Laboratory, Lensfield Rd., Cambridge, UK CB2 1EW.

Experimental

General methods

All chemicals were used as received without further purification. Infrared spectra were recorded as KBr discs, solid state ultraviolet/visible spectra using a KBr pellet matrix. C, H, N and Cl analysis was by the University of East Anglia Elemental Analysis Service. Magnetisation studies were performed on a Quantum Design MPMS SQUID magnetometer. Field cooled measurements ($H = 100$ G) were made from 1.8 to 300 K, while magnetisation curves were obtained for fields up to 10 kG at 5, 8, 9, 10, 12, and 20 K. To ensure an orientationally averaged response a ground powder sample was set in an eicosane matrix. The sample susceptibility was corrected for the underlying diamagnetism using a value of -139×10^{-6} cm^3 mol^{-1} calculated from Pascal's constants.[10] TGA and DTA measurements were made under a H_2/N_2 atmosphere in the range 300 to 1150 K with a heating rate of 10 K min^{-1}.

Synthesis of $Na_2Co_2(C_2O_4)_3(H_2O)_2$, 1

Sodium oxalate (0.835 g, 6.23 mmol) was added to a solution of cobalt(II) chloride hexahydrate (0.519 g, 2.18 mmol) in distilled water (8 cm^3). Sodium chloride (5.121 g, 87.54 mmol) was added to the resulting pink suspension and the mixture heated to 225 °C for 2.5 hours in a 23 cm^3 capacity Teflon-lined autoclave followed by slow cooling to room temperature. Water (200 cm^3) was added to dissolve the soluble salts. Filtration yielded the product **1** as dark purple crystals (0.460 g, 0.99 mmol, 91%). Calc. for $C_3H_2O_7CoNa$: C, 15.53; H, 0.87%. Found: C, 15.65; H, 0.69%; Cl, not detected. IR (KBr, cm^{-1}): 3337s (br) (ν_{OH}), 3077s (br) (ν_{OH}), 1682 (sh), 1636s (ν_{CO_2}), 1609 (sh), 1471m, 1368w, 1313s, 1069w (br), 913w, 817m, 786m, 715m (br), 616m (br), 516w, 497m, 474m, 444w and 411w. UV/visible (KBr, nm); 478 (sh), 546, ≈650 (br) and 664 (possibly due to $CoBr_4^{2-}$ impurity formed in KBr pellet preparation as the intensity of this peak increases with increased grinding of the sample with KBr).

X-Ray crystallography

Data were collected at room temperature on a Rigaku AFC7R diffractometer using Mo-Kα radiation, $T = 293(2)$ K. $C_6H_4Co_2Na_2O_{14}$, $M = 231.97$, monoclinic, space group $P2_1/c$, $a = 5.864(4)$, $b = 15.723(6)$, $c = 6.963(3)$ Å, $\beta = 100.36(4)°$, $V =$

 DOI: 10.1039/b005494l

631.5(2) Å^3. 1215 Reflections were collected of which 1104 were unique (R_{int} = 0.0190). An empirical absorption correction was applied (μ = 2.780 mm^{-1}) . The structure was solved by direct methods and all non-hydrogen atoms were refined anisotropically using full-matrix least squares on F^2. Hydrogen atoms were located in the Fourier difference map and refined isotropically. The final refinement gave $R1 = 0.0211$ ($F > 4\sigma(F)$), $wR2 = 0.0579$ (all data). The maximum and minimum residual electron densities were 0.309 and −0.272 e Å^{-3}.

CCDC reference number 186/2164.

See http://www.rsc.org/suppdata/dt/b0/b005494l/ for crystallographic files in .cif format.

Results and discussion

As part of our search for new transition metal oxalates we have been looking at the products of hydrothermal reactions of various binary and ternary mixtures. In this case reactions were systematically performed across the NaCl/$CoCl_2$/$Na_2C_2O_4$ compositional phase diagram. Large purple crystals of the compound $Na_2Co_2(C_2O_4)_3(H_2O)_2$ **1** were obtained from hydrothermal reactions where the molar ratio of NaCl : $CoCl_2$ was in excess of 40 : 1. No other new solid phases were found in reactions using these components but employing 20 equivalents of NaCl yields α-$Co(C_2O_4)(H_2O)_2$ which is isostructural with the iron(II) mineral humboldtine. The formation of cobalt(II) oxalate dihydrate across a large portion of the reaction composition phase diagram parallels similar findings for the analogous iron chemistry and is further evidence of the stability of this phase. Extensive investigations have also been performed on systems where sodium chloride is replaced by other alkali or alkaline earth metal chlorides. No new or analogous phases were observed except in the barium system.[11] The requirement for a very high concentration of sodium ions in the reaction mixture shows that the chemical potential of Na^+ in **1** is very high. An important point to note is that the solvation properties of concentrated solutions (in this case approximately 10 M NaCl at 225 °C) will be very different from that of pure water or indeed dilute solutions; this is crucial in determining which phase is thermodynamically most stable under these synthetic conditions.

The structure of compound **1** consists of an extended cobalt(II) oxalate network containing one cobalt(II) environment and two types of oxalate ion each of which bridges two cobalt atoms (Fig. 1). One of the oxalates sits on an inversion centre and co-ordinates in a classical symmetrical chelating fashion. The second type of oxalate bridges two cobalt ions in an unsymmetrical fashion with one chelating and one monodentate interaction. The two cobalt atoms bridged in this way are related by a simple translation along the *a* axis giving rise to a ladder structure (Fig. 2). Each cobalt atom has approximately octahedral co-ordination with two chelating oxalates (one of each type) in a *cis* geometry. The remaining two co-ordination sites are occupied by water and an oxygen from an oxalate bonded in a monodentate fashion. The presence of *cis* chelating ligands gives rise to a chiral environment for the cobalt atoms. The metal centres on opposite sides of the ladder have opposite chirality; all Δ down one side and all Λ down the other. This topology for a metal oxalate has been previously reported[12] in the compound $Cs_2Mn_2(C_2O_4)_3(H_2O)_3$ however the materials are not isostructural and contain different quantities of water.

Bond distances and angles (Table 1) are all normal with the cobalt co-ordination sphere showing a tetragonal elongation along the side of the ladder. The largest deviation from an ideal octahedral geometry predictably involves the chelating oxalates. The sodium ions are in a very irregular seven-co-ordinate geometry with Na–O bond lengths in the range 2.305(2) to 2.774(2) Å. The co-ordination environment contains both end-on and side-on chelating oxalates, unidentate oxalates and a water molecule. These irregular polyhedra share two corners (due to the presence of water bridges) forming infinite chains. The water molecules also form hydrogen bonds with atoms in adjacent ladders.

Table 1 Selected bond lengths (Å) and angles (°) for compound **1**

Co1–O1	2.094(2)	C3–O5	1.261(3)
Co1–O2A	2.063(2)	C3–O6	1.235(3)
Co1–O3	2.118(2)		
Co1–O4A	2.168(2)	O5A–Co1–O2A	168.81(8)
Co1–O5A	2.053(2)	O5A–Co1–O7	97.72(9)
Co1–O7	2.086(2)	O2A–Co1–O7	93.00(8)
Na1–O1′	2.359(2)	O5A–Co1–O1	89.06(8)
Na1–O2′	2.725(2)	O2A–Co1–O1	80.51(7)
Na1–O3′	2.774(2)	O7–Co1–O1	172.00(8)
Na1–O3	2.549(2)	O5A–Co1–O3	84.23(8)
Na1–O5A	2.329(2)	O2A–Co1–O3	99.28(8)
Na1–O6	2.305(2)	O7–Co1–O3	88.72(8)
Na1–O7	2.484(2)	O1–Co1–O3	87.75(9)
C1–C1A	1.540(5)	O5A–Co1–O4A	78.40(7)
C1–O1	1.255(3)	O2A–Co1–O4A	98.91(8)
C1–O2	1.255(3)	O7–Co1–O4A	87.66(9)
C2–C3	1.545(4)	O1–Co1–O4A	97.90(9)
C2–O3	1.254(3)	O3–Co1–O4A	161.61(8)
C2–O4	1.254(3)		

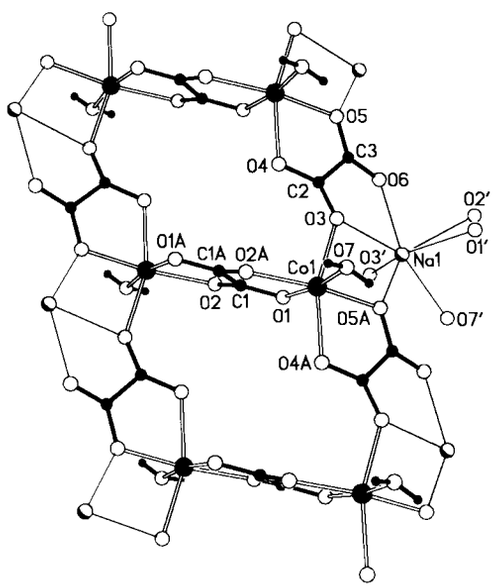

Fig. 1 The asymmetric unit and selected symmetry generated atoms showing the two bridging modes of the oxalate ions. The linkage forming the rungs of the ladder has a Co···Co distance of 5.393(1) Å, the bridge forming the side of the ladder a distance of 5.864(1) Å. The shortest inter-ladder pathway is 5.055(1) Å.

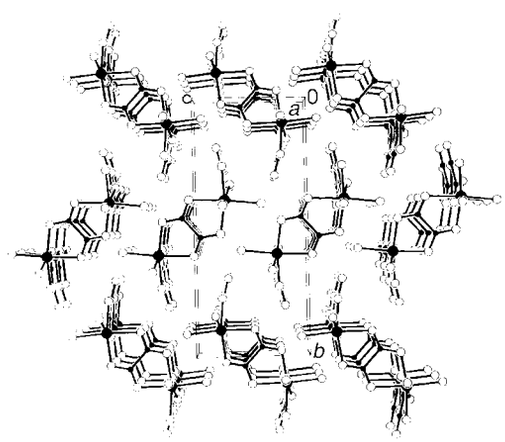

Fig. 2 A packing diagram (sodium ions omitted) showing the relationship between neighbouring ladders.

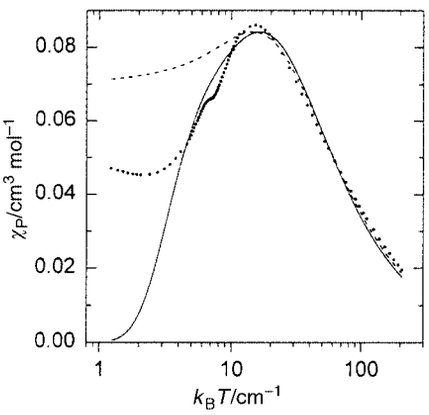

Fig. 3 Semi-log plot of the magnetic susceptibility of compound **1** as a function of thermal energy. The data are represented by dots, the solid line is a best fit for a simple $S = 3/2$ dimer, and the dashed line is the best fit for the chain model obtained using Fisher's equation.

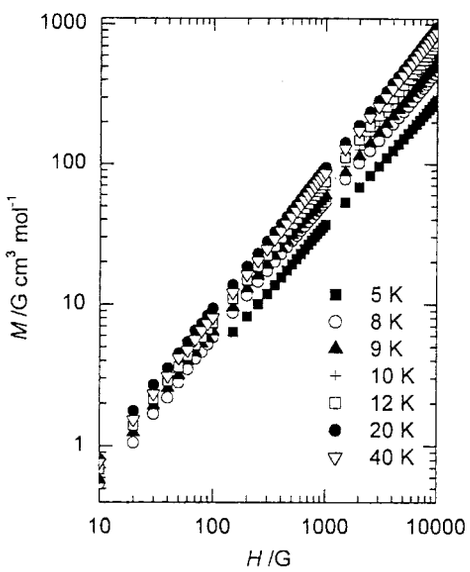

Fig. 4 Magnetisation as a function of field for a range of temperatures across T_N at ≈9 K. The log–log scale demonstrates linearity over a wide range of fields.

Magnetic behaviour

The molar susceptibility of compound **1** as a function of temperature is shown in Fig. 3. The plot shows a broad hump with a maximum at about 21 K and a narrow shoulder on the low temperature side. The position of this inflexion has been determined to be at 9 K by inspection of the derivative curve. As the temperature is lowered towards zero χ levels off to a finite value. The high temperature data (between 40 and 300 K) can be well fitted by the Curie–Weiss law, with $C = 4.86$ cm^3 K mol^{-1} and $\theta = -36$ K. Plotting the effective molecular moment, $\mu_{eff}(T)$, yields a room temperature value of $6.9\mu_B$ which decreases continually on cooling reaching $0.8\mu_B$ by 2 K. The room temperature value compares well with the calculated spin only moment for two $S = 3/2$ ions of $7.74\mu_B$. Attempts to fit the data[13] by a simple axial splitting parameter, D, were unsuccessful suggesting that the gross behaviour is not determined by zero field splittings. Exchange interactions must therefore also contribute to the bulk susceptibility of **1**. A broad maximum in $\chi(T)$ is often associated with short-range antiferromagnetic correlations which are common in materials with a low-dimensional magnetic character. The narrow feature at about 9 K and the finite value of χ as T approaches 0 K are due to a phase transition to an ordered 3-dimensional antiferromagnetic state.

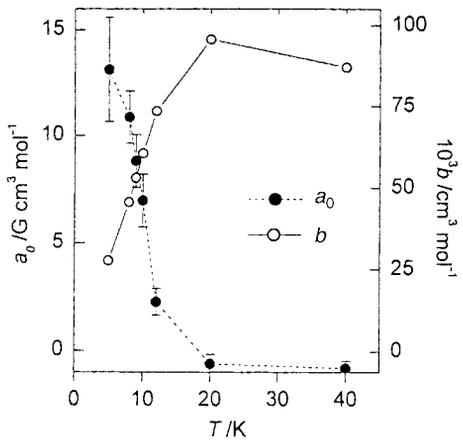

Fig. 5 The temperature dependence of the fitted parameters a_0 and b for the high field data (see main text for details).

The field dependence of the magnetisation was measured for a range of temperatures across the transition at 9 K (Fig. 4). The log–log plot shows the behaviour to be approximately linear for all temperatures and fields. The magnetisation in the high field region (1 and 10 kG) is well fitted by a linear model but deviations are apparent at lower fields. Taking a phenomenological approach the high field data were fitted by the function $M = a_0 + bH$ (Fig. 5). The value of $b(T)$ simply mirrors the susceptibility but the sudden change in $a_0(T)$ at ≈9 K supports the notion of a phase transition at this temperature. The sample shows no hysteresis therefore a_0 is not a spontaneous magnetisation but represents a state of magnetisation that is more readily obtained.

Suitable magnetic models were selected by considering the structural details of compound **1**. In this regard there are three important superexchange pathways: J_1 connects cobalt ions *via* bis-chelating oxalate (the rungs of the structural ladder) producing dinuclear units, J_2 links cobalt ions bridged by the mono-chelating oxalate into linear chains, and in combination J_1 and J_2 form a 2-leg ladder structure. Including a third pathway (J_3) transforms the quasi 1-dimensional ladder structure into a 3-dimensional net. The magnetic susceptibility of **1** depends on the relative magnitudes and signs of all these couplings. Oxalate-bridged cobalt ions typically have exchange couplings[14] of up to -10 cm^{-1} and there are no known examples where the oxalate mediates a ferromagnetic interaction. The pathway between ladders is not formally covalent but involves hydrogen bonds which are known to yield small exchange couplings. Consequently it is likely that $|J_3|$ will be smaller than $|J_1|$ or $|J_2|$.

Ignoring J_3 leaves three important models which depend upon the relative values of J_1 and J_2. In the limit of $J_1/J_2 \rightarrow \infty$ the behaviour will approach that of a simple dimer and if $J_1/J_2 \rightarrow 0$ the behaviour will be more like that of a chain. In intermediate cases the behaviour will be better described as a spin ladder. For each of these scenarios the low dimensional character of the magnetic lattices prevents the onset of long range order with the consequence that at low temperatures these systems have the potential to give interesting quantum phase behaviour.[6]

Each of these antiferromagnetic models exhibits a broad maximum in the susceptibility, as observed for compound **1**, but both the dimer state and the 2-legged ladder (for half-integral spin only) should have a gap in their excitation spectra. Consequently, as T approaches 0 K, χ should also approach zero. The half-integral spin chain has a gapless spectrum and χ should approach a finite value as T approaches zero. In our case the finite value of J_3 leads to a crossover in the effective lattice dimensionality and an accompanying phase transition to an ordered antiferromagnetic state.

Fits of the data in the paramagnetic regime ($13 < T < 300$ K) by the dimer[13] and chain[15] models can be seen in Fig. 3. These give values for the coupling of -5.4 cm^{-1} for the dimer model and -5.3 and -4.2 cm^{-1} for the classical and quantum chain models, respectively. While the gross features of the susceptibility above T_N are reproduced by each of these models, both curves deviate significantly from the observed behaviour. At present there are no simple methods to model the behaviour of an $S = 3/2$ spin ladder ($J_1/J_2 = 1$) in the region of the broad maximum, although this problem is currently receiving much theoretical interest and models for high temperature (series expansions) and low temperature (exponential decay) are known.

The Néel ordering at ≈9 K is associated with an increase in lattice dimensionality from effectively 1-D to a 3-D net. We have modelled this by employing Oguchi's method,[16] which relates T_N and the intra-chain coupling to the inter-chain interaction between an array of loosely coupled simple linear chains. This gives a value of $|J_3| \approx 0.2$ cm^{-1} which we may compare with the result obtained by Troyer *et al.*[9] for an array of spin 1/2 ladders with $J_1 = J_2$, *i.e.* identical rungs. They find that the inter-ladder coupling must exceed a critical value for long range order to occur, specifically $J_3 > 0.11J$. Although it appears that for **1** J_3 is below the critical limit this system deviates from that modelled by Troyer in important respects: it has $S = 3/2$ high spin Co(II), is certainly not a Heisenberg spin system and also $J_1 \neq J_2$. Although the phase transition to a magnetically ordered state rules out the prospect of any interesting quantum phase behaviour, **1** may still provide a useful real example of an antiferromagnetic 2-leg spin ladder at temperatures just above T_N.

Thermal stability

Thermal stability of compound **1** was investigated by TGA. On heating there are two clear decomposition episodes. At 350 °C the sample mass decreases by 8%, consistent with the loss of all water. The relatively high temperature of this event is reasonable since the crystal structure shows that the water is tightly held in the lattice by co-ordination to both cobalt and sodium cations. At about 400 °C a further 34% of the original mass is lost to give a black powder. This phase, which is probably an oxide, shows no further reaction having a constant mass up to 850 °C.

Conclusion

We have again demonstrated the suitability of hydrothermal techniques to form new magnetic materials with extended network structures by the synthesis of compound **1** in a highly concentrated salt solution. This compound has a particularly interesting ladder topology of coupled cobalt(II) ions. Such structures are presently not very common although there is currently much theoretical interest in their low temperature quantum phase behaviour. Unfortunately it appears that inter-ladder exchange in **1** is large enough to cause the onset of 3-D long range ordering below 9 K. Nevertheless it is hoped that for temperatures down to this transition **1** may provide a real example of a $S = 3/2$ spin ladder.

Acknowledgements

We thank Dr Gavin Whittaker for his assistance with TGA measurements. The work was supported by the EPSRC.

References

1 See, for example, *Studies in Soviet Science: Crystallisation Processes under Hydrothermal Conditions*, ed A. N. Lobachev, Plenum, New York, 1973.
2 S. Romero, A. Mossel and J. C. Trombe, *J. Solid State Chem.*, 1996, **127**, 256; P. J. Zapf, D. J. Rose, R. C. Haushalter and J. Zubieta, *J. Solid State Chem.*, 1996, **125**, 182; S. Ayyappan, X. Bu, A. K. Cheetham, S. Natarajan and C. N. R. Rao, *Chem. Commun.*, 1998, 2181; M. Molinier, D. J. Price, P. T. Wood and A. K. Powell, *J. Chem. Soc., Dalton Trans.*, 1997, 4061; P. Amorós, M. D. Marcos, M. Roca, A. Beltrán-Porter and D. Beltrán-Porter, *J. Solid State Chem.*, 1996, **126**, 169; S. H. O. Gutschke, A. M. Z. Slawin and P. T. Wood, *J. Chem. Soc., Chem. Commun.*, 1995, 2197; O. M. Yaghi and H. Li, *J. Am. Chem. Soc.*, 1995, **117**, 10401; C. Livage, C. Egger and G. Férey, *Chem. Mater.*, 1999, **11**, 1546.
3 D. J. Price, A. K. Powell and P. T. Wood, *Polyhedron*, 1999, **18**, 2499.
4 S. O. H. Gutschke, D. J. Price, A. K. Powell and P. T. Wood, *Angew. Chem., Int. Ed.*, 1999, **38**, 1088; A. Distler, D. L. Lohse and S. C. Sevov, *J. Chem. Soc., Dalton Trans.*, 1999, 1805; P. Rabu, P. Janvier and B. Bujoli, *J. Mater. Chem.*, 1999, **9**, 1323; P. Feng, X. Bu and G. D. Stucky, *J. Solid State Chem.*, 1997, **129**, 328; S. O. H. Gutschke, M. Molinier, A. K. Powell, R. E. P. Winpenny and P. T. Wood, *Chem. Commun.*, 1996, 823; J. R. D. DeBord, W. M. Reiff, R. C. Haushalter and J. Zubieta, *J. Solid State Chem.*, 1996, **125**, 186; J. Y. Lu, M. A. Lawandy, J. Li, T. Yuen and C. L. Lin, *Inorg. Chem.*, 1999, **38**, 2695.
5 L. J. DeJongh and A. R. Miedema, *Adv. Phys.*, 1974, **23**, 1.
6 See for example: S. E. Barnes, R. Ballou, B. Barbara and J. Strelen, *Phys. Rev. Lett.*, 1997, **79**, 289; G. Murthy, D. Avoras and A. Auerbach, *Phys. Rev. B*, 1997, **55**, 3104; A. Kitazawa, K. Nomura and K. Okamoto, *Phys. Rev. Lett.*, 1996, **76**, 4038; M. den Nijs and K. Rommelse, *Phys. Rev. B*, 1989, **40**, 4709.
7 T. Barns, E. Dagotto, J. Riera and E. Sanson, *Phys. Rev. B*, 1993, **47**, 3196; H. Tsunetsugu, M. Troyer and T. M. Rice, *Phys. Rev. B*, 1994, **49**, 16078; E. Dagotto, J. Riera and D. Scalapino, *Phys. Rev. B*, 1992, **45**, 5744.
8 D. Arcon, A. Lappas, S. Margadonna, K. Prassides, E. Ribera, J. Veciana, C. Rovira, R. T. Henriques and M. Almeida, *Phys. Rev. B*, 1999, **60**, 4191; C. Rovira, J. Veciana, E. Ribera, J. Tarrés, E. Canadell, R. Rousseau, M. Mas, E. Molins, M. Almeida, R. T. Henriques, J. Morgado, J.-P. Schoeffel and J.-P. Pouget, *Angew. Chem., Int. Ed. Engl.*, 1997, **36**, 2324.
9 M. Troyer, M. E. Zhitomirsky and K. Ueda, *Phys. Rev. B*, 1997, **55**, R6117.
10 See, for example, O. Kahn, *Molecular Magnetism*, Wiley-VCH, Chichester, 1993.
11 D. J. Price, A. K. Powell and P. T. Wood, unpublished work.
12 H. Siems and J. Löhn, *Z. Anorg. Allg. Chem.*, 1972, **393**, 97.
13 C. J. O'Conner, *Prog. Inorg. Chem.*, 1982, **29**, 203.
14 J. Glerup, P. A. Goodson, D. S. Hodgeson and K. Michelson, *Inorg. Chem.*, 1995, **34**, 6255.
15 M. E. Fisher, *Am. J. Phys.*, 1964, **32**, 343; C. Y. Weng, Ph.D. Thesis, Carnegie-Mellon University, 1969.
16 T. Oguchi, *Phys. Rev. A*, 1964, **133**, 1098.